Genes & Diseases (2021) 8, 331–343

Available online at www.sciencedirect.com

ScienceDirect

journal homepage: http://ees.elsevier.com/gendis/default.asp

FULL LENGTH ARTICLE

Dedifferentiated human umbilical cord mesenchymal stem cell reprogramming of endogenous hSDF-1α expression participates in neural restoration in hypoxic-ischemic brain damage rats

Zhou Xiaoqin [a,b,1], Liu Jia [a,b,1], Dai Mengjie [d], Gu Jialu [e], Bi Yang [c], Wang Yuting [a,b], Hu Huajian [a,b], Liu Bo [a,b], Zhang Xiaojun [a,b], Li Zhongyue [a,b], Chen Jie [c], Li Tingyu [c,**], Zhan Xue [a,b,*]

[a] *Department of Gastroenterology, Ministry of Education Key Laboratory of Child Development and Disorders, National Clinical Research Center for Child Health and Disorders (Chongqing), 401122, PR China*
[b] *International Science and Technology Cooperation Base of Child Development and Critical Disorders, Children's Hospital of Chongqing Medical University, Chongqing, 401122, PR China*
[c] *Department of Pediatric Research Institute, Chongqing Key Laboratory of Child Health and Nutrition, Children's Hospital of Chongqing Medical University, Chongqing, 401122, PR China*
[d] *Department of Neonatology, Chongqing Health Center for Women and Children, 400021, PR China*
[e] *Child Health Centre of Northwest Women and Children's Hospital, USA*

Received 13 November 2019; accepted 18 January 2020
Available online 18 February 2020

KEYWORDS
Dedifferentiation;
Human umbilical cord mesenchymal stem cells;
Hypoxic-ischemic brain damage;

Abstract The transplantation of human umbilical cord mesenchymal stem cells (hUC-MSCs) can promote hypoxic-ischemic brain damage (HIBD) nerve repair, but finding suitable seed cells to optimize transplantation and improve treatment efficiency is an urgent problem to be solved. In this study, we induced hUC-MSCs into dedifferentiated hUC-MSCs (De-hUC-MSCs), and the morphology, stem cell surface markers, proliferation and tri-directional differentiation ability of the De-hUC-MSCs and hUC-MSCs were detected. A whole-gene chip was utilized for genome cluster, gene ontology and KEGG pathway analyses of differentially expressed

* Corresponding author.
** Corresponding author.
E-mail addresses: tyli@vip.sina.com (L. Tingyu), zhanxue@hotmail.com (Z. Xue).
Peer review under responsibility of Chongqing Medical University.
[1] Zhou Xiaoqin and Liu Jia were first co-authors.

https://doi.org/10.1016/j.gendis.2020.01.012

Neurorestoration;
Reprogramming;
Stromal cell-derived factor-1

genes. De-hUC-MSCs were transplanted into HIBD rats, and behavioral experiments and immunofluorescence assays were used to assess the therapeutic effect. A lentivirus vector for human stromal cell-derived factor-1 (hSDF-1α) was constructed, and the role of hSDF-1α in the neuroprotective effect and mechanism of De-hUC-MSCs was verified. De-hUC-MSCs displayed similar cell morphology, stem cell surface marker expression, cell proliferation and even three-dimensional differentiation ability as hUC-MSCs but exhibited greater treatment potential *in vivo*. The reprogramming mechanism of hSDF-1α participated in the dedifferentiation process. By successfully constructing a stable hSDF-1α cell line, we found that De-hUC-MSCs might participate in nerve repair through the hSDF-1α/CXCR4/PI3K/Akt pathway. De-hUC-MSCs reprogramming of endogenous hSDF-1α expression may mediate the hSDF-1α/CXCR4/PI3K/Akt pathway involved in nerve repair in HIBD rats.

Introduction

Hypoxic-ischemic brain damage (HIBD) remains a common neurological disease in the neonatal period and has received worldwide attention. HIBD incidence ranges from 1 to 8 and 25 out of every 1000 children born in developed and developing countries.[1] Approximately 10%—60% of children with HIBD in the world eventually die, and unfortunately, approximately 25% of surviving children have long-term neurodevelopmental deficits and disorders.[2]

In recent years, studies by us and others have found that transplantation of human umbilical cord mesenchymal stem cells (hUC-MSCs) offers promising results in HIBD nerve repair.[3—5] However, with the deepening of research, the problems of the low survival rate, low directional differentiation rate and small therapeutic window of hUC-MSCs have become increasingly prominent. Finding suitable seed cells to optimize transplantation schemes and improve treatment efficiency has become a hot topic in the field of MSC transplantation therapy.[6—8]

Dedifferentiation refers to the return of differentiated and mature cells from a relatively well-differentiated state to a naive differentiated or undifferentiated state. It is an ideal approach for tissue regeneration and repair.[9,10] Some studies have reported that dedifferentiated cells exhibit stronger function, dedifferentiated hUC-MSCs improve nerve ability in HIBD rats and dedifferentiated mouse cardiomyocyte cells prompt cardiac function.[11,12] As a new type of seed cell, hUC-MSCs brings new hope to the transplantation therapy field. However, there are only a few studies on dedifferentiated stem cells, and correspondingly, the mechanism is unclear. Thus, it is important to close this gap.

In the current study, we first induce hUC-MSCs into dedifferentiated hUC-MSCs (De-hUC-MSCs) *in vitro* and identify their biological characteristics. Then, the cells were transplanted into HIBD rats to explore their neuroprotective role and possible mechanism.

Materials and methods

Culture and dedifferentiation induction

hUC-MSCs were provided by Chongqing Stem Cell Bank, and their use was approved by the Ethics Committee of Children's Hospital of Chongqing Medical University (Approval number: 024/2013). The hUC-MSCs were inoculated in Dulbecco's modified medium/F12 (DMEM/F12; 1:1; Gibco, USA) containing 10% FBS (Gibco, Australia), 100 units/ml penicillin and 100 μg/ml streptomycin and cultured in an incubator at 37 °C with 5% CO_2. Fresh culture medium was changed every 2—3 days, and when the cells grew to 90% fusion, trypsin/EDTA (Gibco, USA) was used to digest and passage the cells. All cells used in the experiments were from passage 5 to passage 10. According to the mature established dedifferentiation induction method reported by our research group,[3] the hUC-MSCs were preinduced with ATRA (1 μmol/L) for 24 h and washed twice with D-Hank's for 24 h. Then, MNM induction solution (Sigma—Aldrich, USA) was supplied to induce neural differentiation for 24 h. The MNM induction solution was removed, and the cells were carefully washed twice with D-Hank's solution and cultured with complete medium (DMEM/F12 containing 10% FBS) for 24 h to achieve De-hUC-MSCs.

Flow cytometry

hUC-MSCs and De-hUC-MSCs were separately digested with the appropriate amount of trypsin/EDTA to collect the digested cells and were divided into 6 EP tubes, each containing more than 1×10^6 cells per tube. The cells were blocked in serum for 30 min, washed twice with PBS, and resuspended in 100 μL of PBS. IgG1-PE and IgG1-FITC monoclonal antibodies (4A Biotech, Co., Ltd, China) were added to the control tube, and anti-CD29-PE and anti-HLA-DR-FITC; anti-CD34-PE and anti-CD45-FITC; anti-CD105-PE and anti-CD44-FITC; and anti-HLA-ABC-PE and IgG1-FITC (eBioscience or Bioscience, San Diego, CA, USA) antibodies were added to the other 4 tubes, followed by incubation for 30 min. The cells were then washed twice with PBS and analyzed using a FACSCanto II System (BD Bioscience).

Proliferative capacity

hUC-MSCs and De-hUC-MSCs were plated into two 96-well plates at 5×10^3/well. After culture for 24 h, the cells were washed with D-Hank's solution 3 times, 100 μL/well of complete medium was added along the well wall, and 10 μL/well of CCK-8 reagent (DojinDo, Japan) was added. After incubation at 37 °C for 2.5 h, the absorbance at

450 nm was measured and counted as the 0 point, and then, the absorbance at 1, 2, 3, 6, 10, 13 h was measured and calculated.

Induction of tridirectional differentiation

Osteogenesis induction

P3 generation hUC-MSCs and De-hUC-MSCs were induced in complete medium to 80%—90% confluence, and 3×10^5 cells/well were seeded in 6-well plates (precoated with gelatin) and cultured at 37 °C in a 5% CO_2 cell culture incubator. After 24 h, the complete medium was removed, the cells were washed with D-Hank's 3 times, and the medium was replaced with osteogenic induction medium (Cyagen, China), which was changed every 2—3 days. The cells were cocultured for 3 weeks, and then, differentiated cells were identified by alizarin red staining (Cyagen, China).

Adipogenic induction

When P3 generation hUC-MSCs and De-hUC-MSCs fused to 80%—90%, they were digested by trypsin/EDTA and cultured in 6-well plates at 2×10^5 cells/well until reaching 100% confluence (i.e., 3—5 days after maturation). The DMEM/F12 complete medium was removed, the cells were washed 3 times in D-Hank's solution, and the medium was replaced with lipid-inducing A solution (Cyagen, China) and 3 days later with lipid-inducing B (Cyagen, China). After 24 h, liquid A was replaced again, and then circulated 3—5 times. Finally, liquid B was maintained for 7 days and replaced once every 3 days. Oil red O staining (Cyagen, China) was applied for lipid identification.

Chondrogenic differentiation

hUC-MSCs and De-hUC-MSC were plated at 2×10^6 cells/well in 6-well plates and cultured in complete medium for 24 h, and then, the medium was replaced with complete chondrogenic induction solution (Cyagen, China). After 2 days of cultivation, the cells were gently washed twice with incomplete osteogenic induction medium, returned to the complete induction medium for another 28 days and then stained with alcian blue (Cyagen, China).

Microarray analysis

Microarray analysis was performed according to a previously reported protocol.[3] In short, biological replications of hUC-MSCs (1E, 2E, 3E) and De-hUC-MSCs (7E, 8E, 9E) from three different individuals were prepared on a Human Genome U133 plus 2.0 array for full gene analysis. Cluster version 2.11 software was used for hierarchical clustering of the expression profiles, and Affymetrix®NetAffx™Analysis Center software was applied for gene ontology analysis. The screening criteria for differentially expressed genes were as follows: *P* value less than 0.05 and logFC greater than or equal to 1 or less than −1. Differentially expressed genes were selected for further analyses.

RNA extraction and analysis

RNA was extracted using an RNA Extraction Kit (Bioteke Co., Ltd, China), reverse transcription was carried out according to a PrimeScript RT Reagent Kit (Takara, Japan), and the target gene was detected via SYBR-Green real-time PCR (Takara, Japan). Samples were normalized to the expression level of β-actin. The primer sequences were as follows (see Table 1).

Western blotting

Hippocampal brain tissue was isolated using RIPA buffer containing PMSF (Bioteke Co., Ltd, China). On the basis of the molecular weight of the target protein, different concentrations of separation SDS-PAGE gels (Beyotime, China) and electrical conditions were prepared. Rabbit anti-CXCR4 and rabbit anti-p-PI3k antibodies (Abcam plc, UK) and rabbit anti-PI3k, rabbit anti-AKT and rabbit anti-p-AKT antibodies (Cell Signaling Technology, USA) were prepared. The proteins of interest were visualized using Luminata Crescendo Western HRP substrate (Millipore, Billerica, USA) and the Syngene G-box Imaging System.

Enzyme-linked immunosorbent assay

Cell supernatant and hippocampal brain tissue (protein preparation refers to western blotting) were collected. hSDF-1α production was examined using commercially available ELISA Kits (Raybiotech, USA). The experimental procedure was performed in accordance with the manufacturer's protocol. The optical density at 450 nm was recorded using a microtiter plate reader (Thermo, USA).

Establishment of sihSDF-1α-De-hUC-MSCs and AdhSDF-1α-De-hUC-MSCs

According to the CXCL12 (NM_199168) cDNA sequence, the sihSDF-1α and AdhSDF-1α lentivirus vectors were constructed by Neuron Biotech (Shanghai, China). De-hUC-MSCs were inoculated into 24-well plates at 2×10^4 cells/

Table 1 Primer sequence for the target genes.

Gene name	Accession number	Sequence	PCR product
Human Stromal cell-derived factor-1 (hSDF-1α)	NM199168	5′-GCCGCACTTTCACTCTCC-3′ 5′-GGCTCCTACTGTAAGGGTTCC-3′	393 bp
Human β-actin	X00351.1	5′-GTGAAGGTGACAGCAGTCGGTT-3′ 5′-GAGAAGTGGGGTGGCTTTTAGGA-3′	159 bp

well, MOI 10 (AdhSDF-1α lentivirus vectors) and MOI 20 (sihSDF-1α lentivirus vectors) were selected as the optimum concentration by exploring different puromycin and MOI gradients. A single sihSDF-1α infected De-hUC-MSC (represented by SihSDF-1α) or AdhSDF-1α infected De-hUC-MSCs (represented by AdhSDF-1α) was seeded into a 96-well plate to obtain a stable cell line, which was expanded for further experiments.

Rat HIBD model and cell transplantation

A total of 80 SPF SD rats were provided by Chongqing Medical University, and their use was approved by the Ethics Committee of Children's Hospital of Chongqing Medical University (Approval number: 024/2013). The HIBD model was established according to the Rice model, and the cell transplantation was performed according to our previous paper.[3,13] Briefly, five days after establishment of the HIBD model in SD rats (12 days of age), the rats were fixed to a stereotaxic brain locator, and the anterior fontanel was exposed. Then, 5 μL of 2×10^5 cells was injected into the rat at a speed of 1 μL/min. The injection was located 1.1—1.2 mm after the anterior fontanel, 1.4 mm to the left side and 3.5—4.0 mm in depth. Needles were left for several minutes and then slowly removed. The wound was disinfected, and the skin was sutured. SDF-1α (Peprotech, China) was dissolved and resuspended in sterilized PBS to 1000 ng/ml, and the intracranial injection volume was 5 μL.

Histopathology and immunofluorescence

Two days after cell transplantation, the head of the rats was severed, and the left brain tissue was removed and fixed in 4% paraformaldehyde for 1—3 days. For dehydration, 30% sucrose paraformaldehyde was applied. Paraffin sections, 4-μm thick, were prepared, and morphological and histopathological observations were carried out under a light microscope after HE staining. For double-immunofluorescence labeling, brain tissue was sectioned to 15 μm after dehydration, and these sections were immunostained with monoclonal mouse anti-BrdU (Sigma—Aldrich, USA), rabbit anti-Nestin (Santa Cruz, USA), rabbit anti-CD31 (Servicebio, China), and mouse anti-NeuN (Servicebio, China) antibodies at 4 °C for 20 h. The primary antibodies were visualized using Alexa Fluor 488 chicken anti-mouse IgG and Cy3-conjugated Affinipure goat anti-rabbit IgG. Laser scanning confocal microscopy (Nikon, Japan) was applied to capture images.

Morris water maze test

The Morris water maze test was performed 4 weeks after the intracranial injection and was divided into three stages lasting 6 days. On Day 1, the visual platform test was conducted: rats underwent four trials of 60 s in four quadrants, and the time (escape latency) and distance (path length) required to locate the platform were recorded. On Days 2—5, hidden platform training was performed: the rats found a platform within 60 s, and software automatically recorded the event. If the platform was not found, the rats were placed on the platform for 20 s to enhance their memory. The rats were trained four times per day, with an interval of 15—20 min between the two training sessions, for four consecutive days. In the probe trial test (Day 6), the number of times the rats crossed the platform within 60 s was recorded. The time, distance and number of attempts required for rats to find the platform in three periods were statistically analyzed.

Object-in-place task

The experimental details and analysis methods were based on previously published articles.[3] In short, four weeks after cell transplantation, the experimental rats in each group were subjected to an object-in-place experiment. During the adaptation period, the rats were acclimated to the environment for 10 min. On the 3rd day, the rats were placed in a cylinder to explore different toys in the four corners for 5 min. After 5 min of rest, the toys in the exchanged positions (two of them) were again explored for 3 min. The exploration time spent on the four toys and on the two toys in exchanged positions and the two toys in unexchanged positions of every experimental rat was recorded, and the ratio was calculated.

Statistical analysis

The results are presented as the mean ± SD. One-way analysis of variance (ANOVA) was used for multivariate data analysis, and Student's t test was used for statistical analysis. A value of $P < 0.05$ was considered to indicate significance.

Results

Identification of hUC-MSCs and De-hUC-MSCs

Both hUC-MSCs and De-hUC-MSCs displayed spindle-like, spiral and adherent growth. Their proliferation ability was strong, with the ability to cover a 75 cm^2 culture flask in 3—5 days (Fig. 1A and B). Flow cytometry was used to detect the expression of surface markers on hUC-MSCs and De-hUC-MSCs (Fig. 1C and D). The results showed that CD29, CD44, CD105 and HLA-ABC were positively expressed in both cells, while the cells were negative for HLA-DR, CD34 and CD45 expression, suggesting that both hUC-MSCs and De-hUC-MSCs express surface antigens of hMSCs. The proliferation curves constructed with CCK8 proliferation experiment results demonstrated that the cell growth phase was 1—10 days and the logarithmic growth phase was 3—6 days, with a downward trend after 10 days. The hUC-MSCs and De-hUC-MSCs showed a similar proliferation capacity (Fig. 1E). Osteogenic, adipogenic, and chondrogenic differentiation experiments were used to detect the tridirectional differentiation ability of the cells. After osteogenic induction, the cells showed aggregation and mineralized nodules, and calcified matrix deposits were seen with alizarin red staining. Vacuolar lipid droplets with enhanced refraction were observed after lipogenic

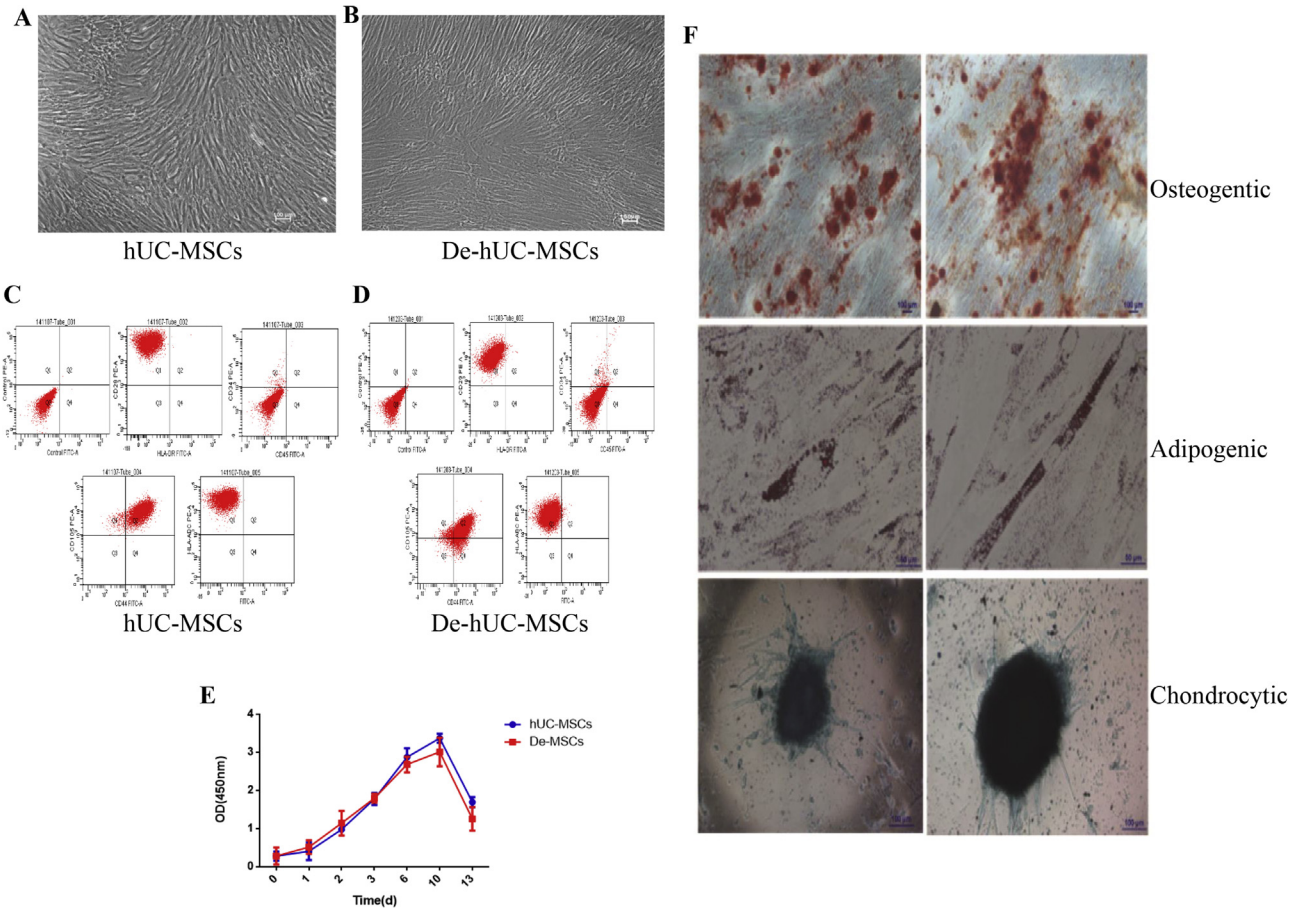

Figure 1 The basic biological characteristics of hUC-MSCs and De-hUC-MSCs. **(A—B)** Morphology of hUC-MSCs and De-hUC-MSCs determined by light microscopy (scale bar = 200 μm). **(C—D)** Flow cytometry analysis of surface markers on hUC-MSCs and De-hUC-MSCs. **(E)** Proliferation ability of hUC-MSCs and De-hUC-MSCs determined using CCK8 assays (the data represent three repetitions). **(F)** hUC-MSC and De-hUC-MSC differentiation into osteoblasts and adipogenic, chondrocytes.

induction. The cells grew flat and round, adhered to the wall, aggregated, and stained positive for chondrocyte characteristics (Fig. 1F), suggesting that both hUC-MSCs and De-hUC-MSCs had the tri-directional differentiation ability of hMSCs. According to the above results, De-hUC-MSCs had stem cell properties similar to those of hUC-MSCs.

The whole-gene expression pattern of hUC-MSCs and De-hUC-MSCs

To further explore the biological characteristic of hUC-MSCs and De-hUC-MSCs, a whole-gene chip was used for detection. According to the screening criteria for differentially expressed genes (briefly, the expression was altered by at least two-fold), there were 693 genes differentially expressed between the two groups, of which 326 were differential high-expression genes and 367 were differential low-expression genes. The differentially expressed genes were analyzed by genome cluster analysis (Fig. 2A). It can be seen from the cluster diagram that hUC-MSCs reprogrammed differential gene expression during the process of dedifferentiation. Gene ontology and KEGG pathway analyses were employed to assess the biological function and possible signaling pathways involved in the dedifferentiation process. SDF-1α is a gene known to participate in the cytokine—cytokine receptor interaction pathway (Fig. 2B and C). Additionally, it was found that SDF-1α was the most differentially expressed gene between De-hUC-MSCs and hUC-MSCs, and the same result was verified by RT-PCR (Fig. 2D and E), indicating that the dedifferentiation process mediates reprogramming of SDF-1α expression, which may take part in the biological function of De-hUC-MSCs.

Therapeutic effect of hUC-MSCs and De-hUC-MSCs in HIBD rats *in vivo*

The above results revealed that hUC-MSCs and De-hUC-MSCs have similar biological properties. How do they differ in therapeutic potential? To answer this question, hUC-MSCs and De-hUC-MSCs were transplanted into the lateral ventricle of HIBD rats. A $Nestin^{+}$ (red)/$BrdU^{+}$ (green) double-label immunofluorescence assay was used to

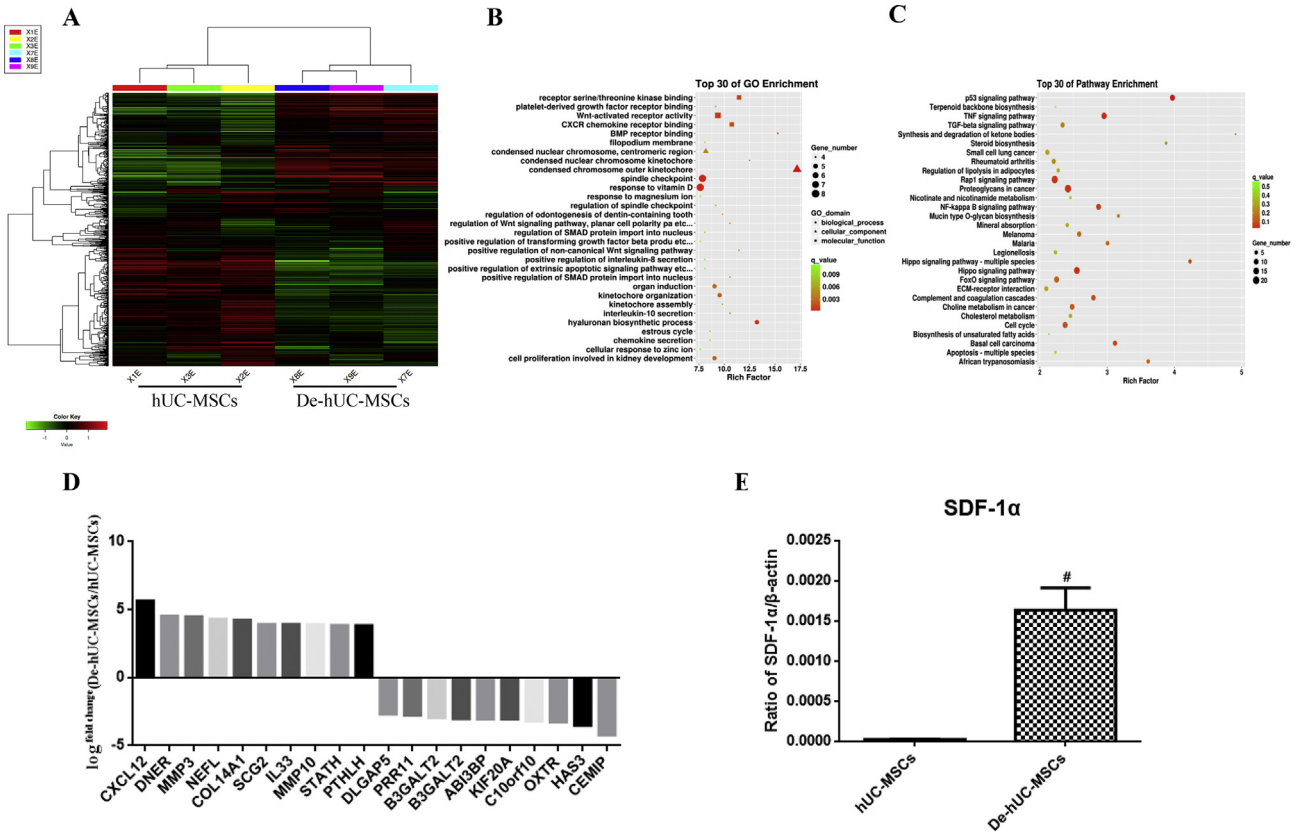

Figure 2 Analysis of gene expression differences in hUC-MSCs and De-hUC-MSCs with a gene expression profiling array. **(A)** Cluster analysis of the top 1200 genes with the greatest difference between hUC-MSCs and De-hUC-MSCs. **(B)** Illustration showing the top 30 Gene ontology enrichment results. **(C)** List of the top 30 KEGG pathway enrichment results. **(D)** The top 10 and the last 10 genes with expression differences between hUC-MSCs and De-hUC-MSCs in the gene chip. **(E)** Real-time PCR verified hSDF-1α gene expression in hUC-MSCs and De-hUC-MSCs ($^{\#}P < 0.001$, De-hUC-MSCs *vs.* hUC-MSCs; Student's *t* test).

observe neurogenesis in the hippocampus (Fig. 3A and B). It can be seen that the number of positive cells in the De-hUC-MSCs group was higher than in the PBS group and hUC-MSC group, and the differences were significant. A Morris water maze behavioral experiment was used to examine the effects of hUC-MSC and De-hUC-MSCs transplantation on the learning ability and spatial memory function of HIBD rats. On the first day of the visible platform test (Fig. 3C and D), no significant difference in the distance and time needed to find the platform was observed among rats in the PBS group, hUC-MSC group and De-hUC-MSC group. During the hidden platform training on days 2—5 (Fig. 3E), as the number of training days increased, the time needed by the rats in each group to find the platform decreased. The De-hUC-MSCs transplantation group took the shortest time to find the platform, and the difference was statistically significant. In the probe trial tests (Day 6) (Fig. 3F), the frequency of platform finding in the De-hUC-MSCs group was higher than in the hUC-MSC transplantation group and PBS group. ELISAs were used to evaluate the rat brain tissue in the hippocampal region and showed that hSDF-1α was highly differentially expressed in the De-hUC-MSCs group (Fig. 3G). These results suggest that transplantation of De-hUC-MSCs can promote neurogenesis and learning and memory function in HIBD rats more effectively than hUC-MSC transplantation and that hSDF-1α may play an important role.

Construction of AdhSDF-1α-De-hUC-MSCs and SihSDF-1α-De-hUC-MSCs cell lines

To demonstrate the effect of SDF-1α, it was necessary to construct a stable expression cell line. By screening the MOI value and infection time used to produce lentivirus-infected De-hUC-MSCs and observing the fluorescence expression with an inverted fluorescence microscope, stable De-hUC-MSCs strains with a greater than 80% infection rate were obtained by selecting an MOI of 20 in the SihSDF-1α group and an MOI of 10 in the AdhSDF-1α group (Fig. 4A). RT-PCR results showed that the expression of hSDF-1α was alleviated after De-hUC-MSCs were infected with SihSDF-1α but was promoted in the AdhSDF-1α group, and the difference was statistically significant (Fig. 4B). Meanwhile, the

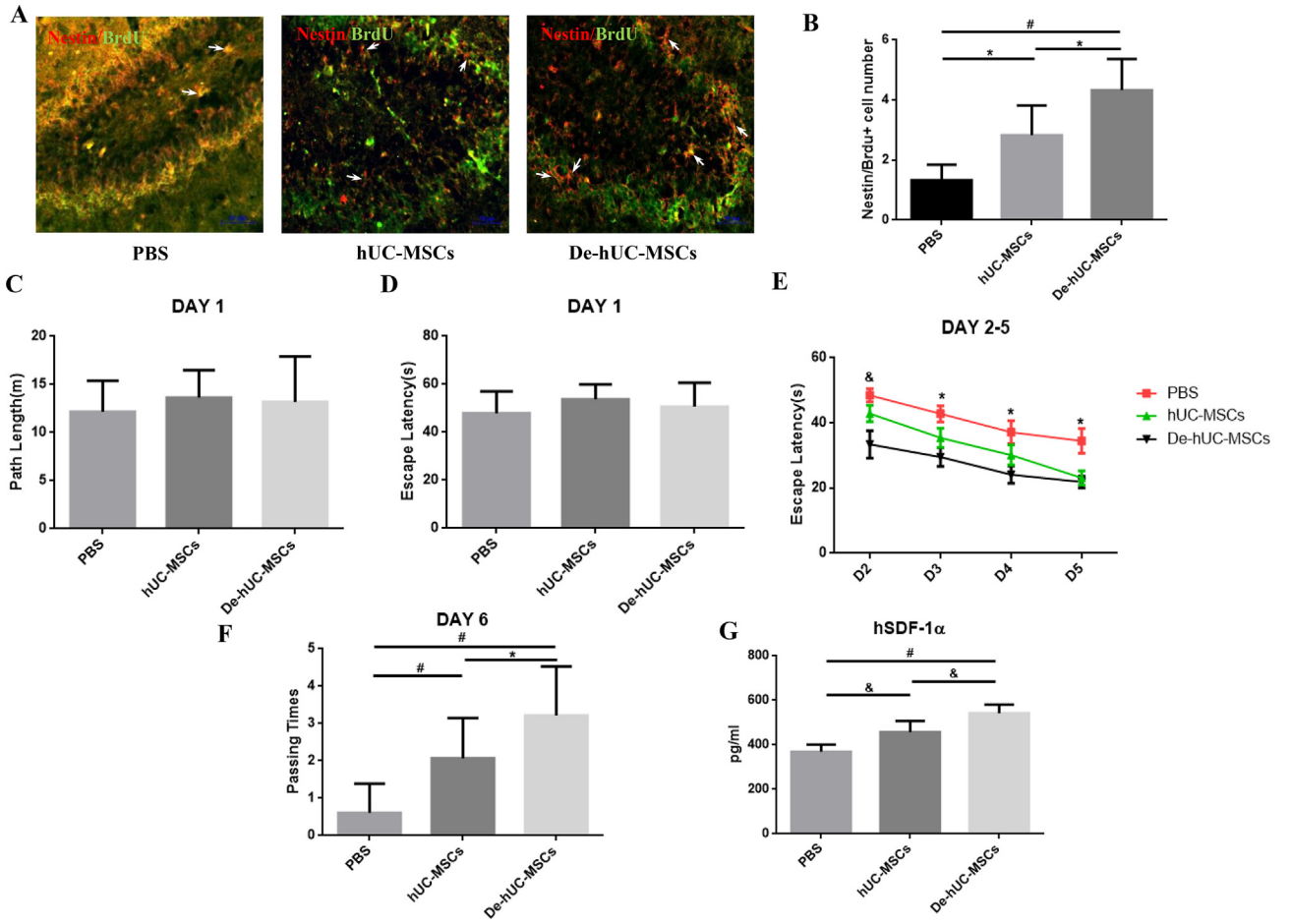

Figure 3 Comparison of neural repair ability between hUC-MSCs and De-hUC-MSCs in vivo. **(A)** Neurogenesis evaluated via immunofluorescence in the hippocampus of HIBD rats following cell transplantation. **(B)** Quantification of the number of Nestin^{+}/BrdU+cells in rat hippocampus tissues ($^{\#}P < 0.001$, De-hUC-MSCs *vs*. PBS; $^{*}P < 0.05$, hUC-MSCs *vs*. PBS and De-hUC-MSCs *vs*. hUC-MSCs; one-way ANOVA). **(C—F)** The spatial learning and memory ability of HIBD rats detected in a Morris water maze test **(C—D)** Path length and escape latency of rats in the PBS ($n = 15$), hUC-MSC ($n = 19$) and De-hUC-MSC ($n = 14$) groups during visual training (DAY 1) on the Morris water maze ($P > 0.05$; one-way ANOVA). **(E)** The escape latency of rats in the four groups on training days 2—5 ($^{\&}P < 0.01$, D2, PBS *vs*. De-hUC-MSCs; $^{*}P < 0.05$, D3-D5, PBS *vs*. De-hUC-MSCs; two-way ANOVA). **(F)** The number of times passing the platform in the four groups on day 6 ($^{\#}P < 0.001$, PBS *vs*. De-hUC-MSCs; $^{\#}P < 0.001$, PBS *vs*. hUC-MSCs; $^{*}P < 0.05$, hUC-MSCs *vs*. De-hUC-MSCs; one-way ANOVA). **(G)** Detection of hSDF-1α expression in the hippocampus via ELISA ($^{\#}P < 0.001$, PBS *vs*. De-hUC-MSCs; $^{\&}P < 0.05$, PBS *vs*. hUC-MSCs and hUC-MSCs *vs*. De-hUC-MSCs; one-way ANOVA).

supernatant of infected cells was collected, and the hSDF-1α level was detected by ELISA. The same results were received (Fig. 4C), indicating that AdhSDF-1α-De-hUC-MSC (represented by AdhSDF-1α) and SihSDF-1α-De-hUC-MSC (represented by SihSDF-1α) cell lines were successfully constructed.

Exploring the role of hSDF-1α from De-hUC-MSCs in nerve repair

To evaluate whether De-hUC-MSCs participate in recovery of learning ability and spatial memory function of HIBD rats through hSDF-1α, De-hUC-MSCs, GFP, AdhSDF-1α, SihSDF-1α and exogenous SDF-1α were transplanted into HIBD rats. The effects of the five treatments on learning and memory function of HIBD rats were examined using a Morris water maze. On the first day, there was no significant difference in the path length or the escape latency among the five groups (Fig. 5A and B). After 2—5 days of hidden platform training, the time spent to find the platform in the AdhSDF-1α group was less than that in the SihSDF-1α group, and the difference was statistically significant (Fig. 5C). In the probe trial test on the 6th day, the frequency of finding the platform was significantly higher in the AdhSDF-1α group than in the other four groups (Fig. 5D). An object-in-place behavioral experiment was used to examine spatial configuration memory. As shown in Fig. 5E, rats in the AdhSDF-1α group had higher ability to explore new objects than rats in other groups, and the difference was statistically significance. The above results indicate that De-hUC-

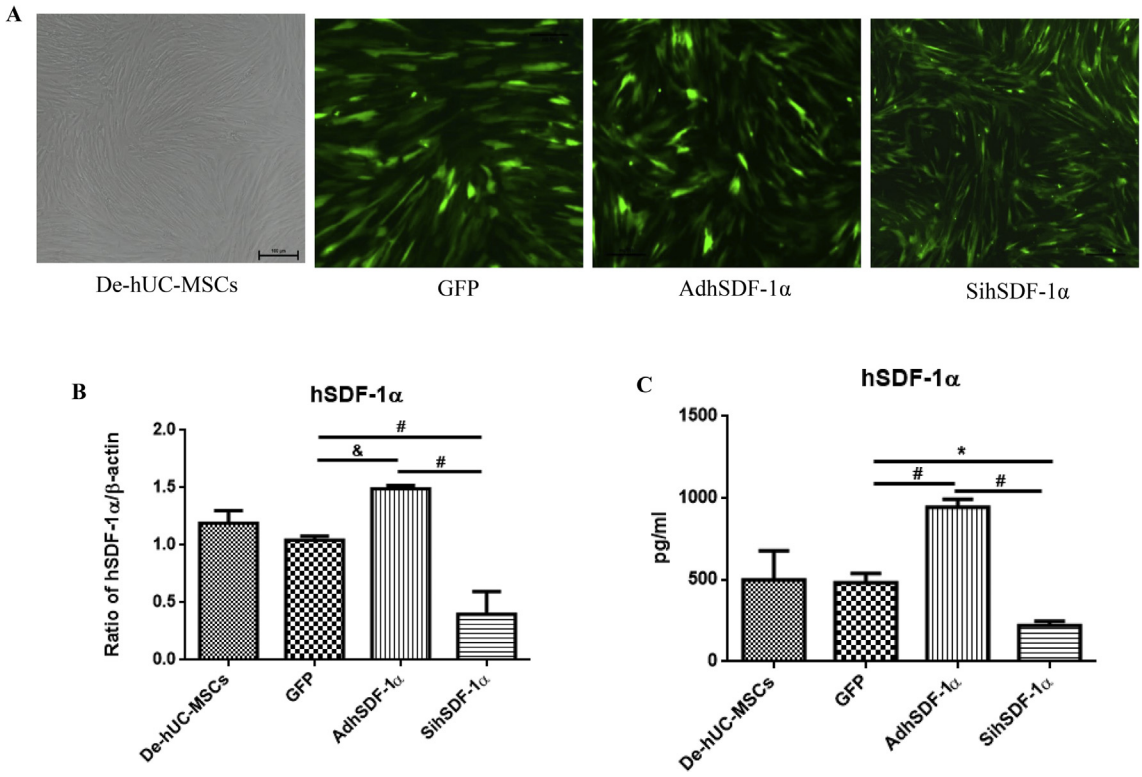

Figure 4 Construction of hSDF-1α stably transfected cell line. **(A)** Morphology of the De-hUC-MSC, GFP, AdhSDF-1α, SihSDF-1α group cells under a fluorescence microscope (scale bar = 100 μm). **(B)** hSDF-1α mRNA expression in the transfected cell groups detected by real-time PCR ($^{\&}P < 0.01$, AdhSDF-1α *vs.* GFP; $^{\#}P < 0.001$, SihSDF-1α *vs.* GFP; $^{\#}P < 0.001$, AdhSDF-1α *vs.* SihSDF-1α; one-way ANOVA). **(C)** The levels of hSDF-1α in the culture supernatants of the four transfected cell groups ($^{\#}P < 0.001$, GFP *vs.* AdhSDF-1α; $^{*}P < 0.05$, GFP *vs.* SihSDF-1α; $^{\#}P < 0.001$, AdhSDF-1α *vs.* SihSDF-1α; one-way ANOVA).

MSCs may participate in the recovery of learning ability and spatial memory function in HIBD rats through hSDF-1α.

Effect of hSDF-1α from De-hUC-MSCs on angiogenesis and neurogenesis and the possible mechanism

To observe the pathological morphology of rat brain tissue in the De-hUC-MSCs, GFP, AdhSDF-1α, SihSDF-1α and hSDF-1α transplantation groups, HE staining was performed. According to Fig. 6, the tissue was closely arranged, and swelling, nuclear pyknosis and vacuoles were induced in hippocampal cells in the AdhSDF-1α group compared with those in the GFP and SihSDF-1α groups. To measure angiogenesis and neurogenesis, a CD31/BrdU double-labeling immunofluorescence assay was applied, and the results showed that $CD31^{+}$ (red)/$BrdU^{+}$ (green) cells were more abundant in the AdhSDF-1α transplantation group than in the other groups, while fewer were present in the SihSDF-1α group, and the difference was statistically significant (Fig. 7A and B). A $NeuN^{+}$ (red)/$BrdU^{+}$ (green) double-labeling immunofluorescence assay was used to demonstrate neurogenesis. Positive cell counts were significantly different in the AdhSDF-1α and SihSDF-1α groups (Fig. 7C and D). Through Western blot detection of the signaling pathway (Fig. 8), the level of CXCR4, phosphorylated PI3K (p-PI3K) and phosphorylated Akt (p-Akt) protein expression in the AdhSDF-1α group was significantly higher than that in the other four groups. Gray level analysis quantitatively showed the level of differences. However, there were no significant differences in PI3K and Akt expression levels among the groups, suggesting that hSDF-1α from De-hUC-MSCs might advance nerve and vascular repair through the CXCR4/PI3K/Akt pathway, while exogenous administration of hSDF-1α does not play a role in HIBD rats.

Discussion

Cellular dedifferentiation underlies topical issues in biology and indicates that cells are not locked in their differentiated state. Dedifferentiation involves regeneration and somatic cell nuclear transfer, and signifies the withdrawal of cells from a given differentiated state into a 'stem cell'-like state that confers pluripotency.[14] In the current study, we first induced hUC-MSCs to dedifferentiate and found that De-hUC-MSCs displayed a similar cell morphology, stem cell surface marker profile, cell proliferation ability and

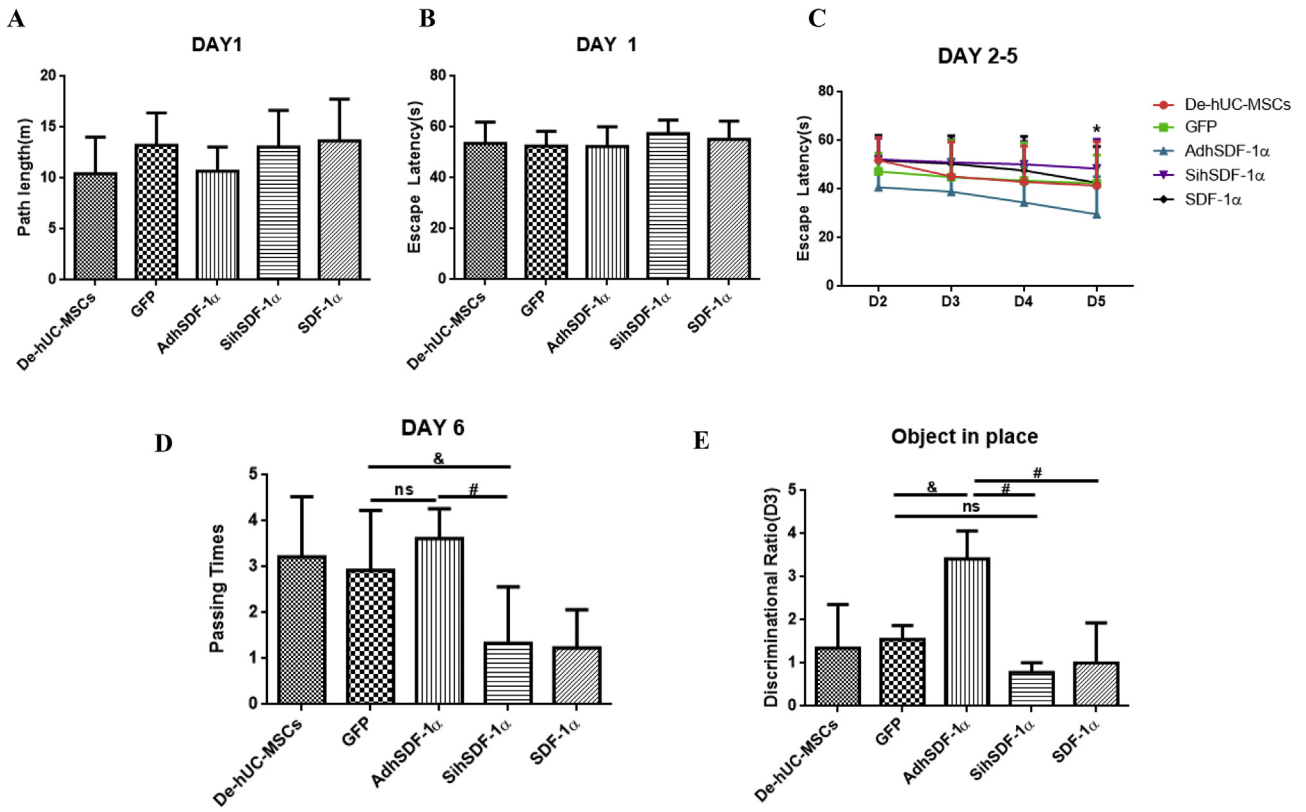

Figure 5 Behavioral test for transplantation of hSDFα-transfected cells into HIBD rats. **(A—D)** Morris water maze for detection of learning and memory ability in the De-hUC-MSC ($n = 10$), GFP ($n = 10$), AdhSDF-1α ($n = 10$), SihSDF-1α ($n = 10$), and SDF-1α ($n = 7$) groups. **(A—B)** Path length and escape latency in the five groups on day 1 ($P > 0.05$, one-way ANOVA). **(C)** Escape latency during training on days 2—5 in the five groups ($^{*}P < 0.05$, AdhSDF-1α *vs*. SihSDF-1α; two-way ANOVA). **(D)** Testing the number of times crossing the platform ($^{ns}P > 0.05$, GFP *vs*. AdhSDF-1α; $^{\&}P < 0.01$, GFP *vs*. SihSDF-1α; $^{\#}P < 0.001$, AdhSDF-1α *vs*. SihSDF-1α; one-way ANOVA). **(E)** The discriminational ratio of the exploration time in the De-hUC-MSC ($n = 7$), GFP ($n = 6$), AdhSDF-1α ($n = 7$), SihSDF-1α ($n = 6$), and SDF-1α ($n = 6$) groups ($^{\&}P < 0.01$, AdhSDF-1α vs. GFP; $^{\#}P < 0.001$, AdhSDF-1α *vs*. SihSDF-1α; $^{\#}P < 0.001$, AdhSDF-1α *vs*. SDF-1α; $^{ns}P > 0.05$, GFP *vs*. SihSDF-1α; one-way ANOVA).

even three-dimensional differentiation ability as hUC-MSCs. As mentioned previously, mature adipocyte-derived dedifferentiated cells exhibit a fibroblast-like morphology and sustain high proliferative activity and multilineage differentiation potential compared with adipose-derived stem cells.[15] Dedifferentiated neural stem cells have the standard phenotype, transcriptome map, metabolic profile, and even differentiation capacity associated with neurons or astrocytes, similar to embryonic stem cells.[16] To verify the function of De-hUC-MSCs in vivo, they were transplanted into an HIBD rat model. Through the Morris water maze behavior experiment and double-label immunofluorescence assay, De-hUC-MSCs demonstrated the function of promoting learning and memory and neurogenesis, which was consistent with a previous study.[11] Similarly, other research groups have also found that transplantation of mature adipocyte-derived dedifferentiated cells significantly increased capillary density in the infarcted area[17] and ameliorated hypoxic-ischemic brain injury.[18]

Reprogramming participates in the dedifferentiation process, which primarily refers to two processes: one is the reversal of differentiated cells to the pluripotent state, and the other is the transformation from one differentiated cell to another. Some studies have shown that many genes reprogramming upregulation or downregulation are involved in dedifferentiation of adipogenic-differentiated MSCs followed by adipogenesis, osteogenesis and chondrogenesis induction.[19,20] In the event of cell reprogramming to dedifferentiate astrocytes into neural stem/progenitor cells, the expression of typical astrocytic markers (GFAP and S100) and neural stem cell markers (nestin, Sox2, and CD133) was reprogrammed.[21] Dedifferentiated adipocytes may participate in functional regulation in the form of secretion by reprogramming cytokine expression (especially TGF-β1).[22,23] In this study, we utilized a whole-gene expression profiling array to explore the genes differentially expressed in the process of dedifferentiation. Overall, 693 genes were differentially expressed between the

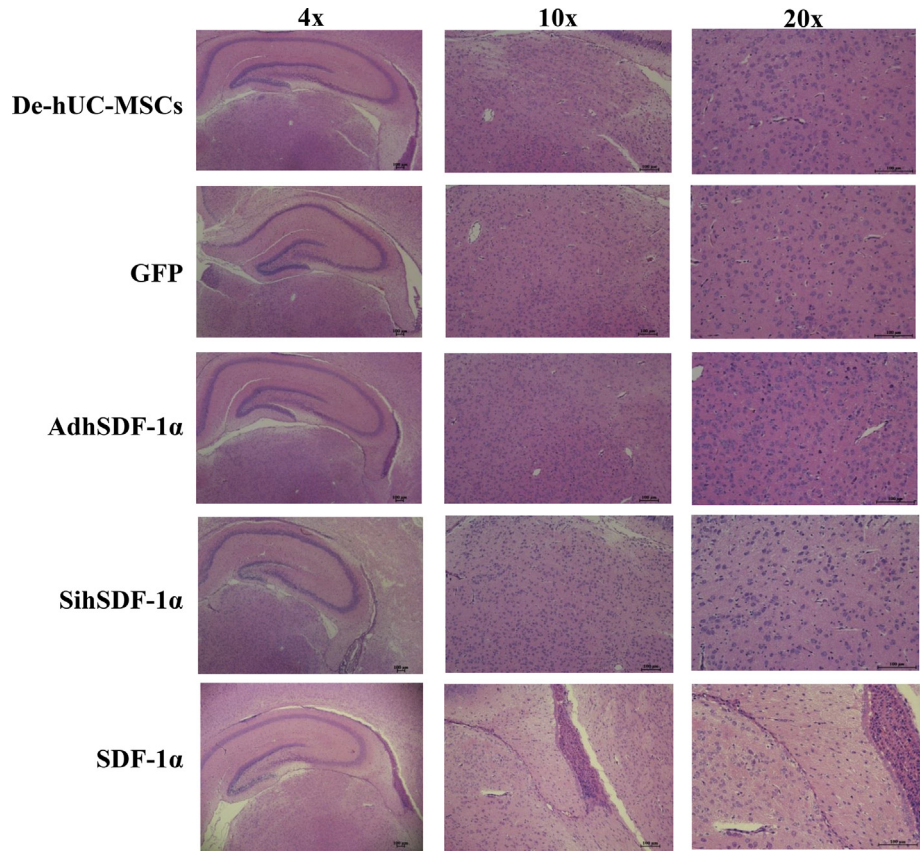

Figure 6 Pathological morphology of brain tissue in each cell transplantation group. A Pathological changes in brain tissue around the lateral ventricle in the De-hUC-MSC, GFP, AdhSDF-1α, SihSDF-1α and SDF-1α groups detected by HE staining (scale bar = 100 μm).

two groups, and hSDF-1α was the most differentially expressed gene between De-hUC-MSCs and hUC-MSCs. Interestingly, KEGG pathway analysis also pointed to hSDF-1α as an exemplary gene involved in the cytokine—cytokine receptor interaction pathway, thereby mediating the process of dedifferentiation. Furthermore, in vivo verification revealed that hSDF-1α was highly expressed in the hippocampal brain tissue of rats in the dedifferentiated transplantation group. Therefore, we speculate that hSDF-1α gene reprogramming may play a role in De-hUC-MSCs.

Stromal cell-derived factor-1 is an important member of the chemokine family. In addition to its classical role in chemotaxis, it is also an important neurovascular factor that plays an important physiological role in ischemic and hypoxic injury of the nervous system. SDF-1α specifically influences neurogenesis and angiogenesis, alleviates inflammation and induces cerebral remyelination, thus improving cognitive functions and spatial perception abilities in HIBD.[24—26] hUC-MSCs secrete hSDF-1 to prompt angiogenesis, gliogenesis and migration, which may extend the therapeutic applicability of stem cells.[27,28] Considering the above results, we found that hSDF-1α may be beneficial for functional recovery after HIBD, and thus, we constructed AdhSDF-1α-De-hUC-MSCs and SihSDF-1α-De-hUC-MSCs cell lines and verified successful construction of the cell lines at the gene and protein levels (Fig. 4). The cell lines were transplanted into HIBD rats, and the function of hSDF-1α in nerve repair was verified by behavioral experiments and histopathological and immunofluorescence assays. By setting up different transplantation groups, the positive and negative directions confirmed that hSDF-1α can promote the recovery of neurovascular function in HIBD. More interestingly, exogenous administration of SDF-1α cannot promote function recovery, suggesting that the endogenous source of hSDF-1α plays a critical role in De-hUC-MSC activity (Fig. 5—7). Our previous study reported that endogenous IL-6 release from MSCs reduced apoptosis of injured astrocytes and mediated a neuroprotective effect in neonatal HIBD rats.[29] hUCB-MSCs enhanced hippocampal neurogenesis and synaptic activity through endogenous secretion of growth differentiation factor-15 (GDF-15), Conversely, exogenous recombinant GDF-15 treatment in both *in vitro* and *in vivo* also enhanced hippocampal neural stem cell proliferation and neuronal differentiation.[30] Combined

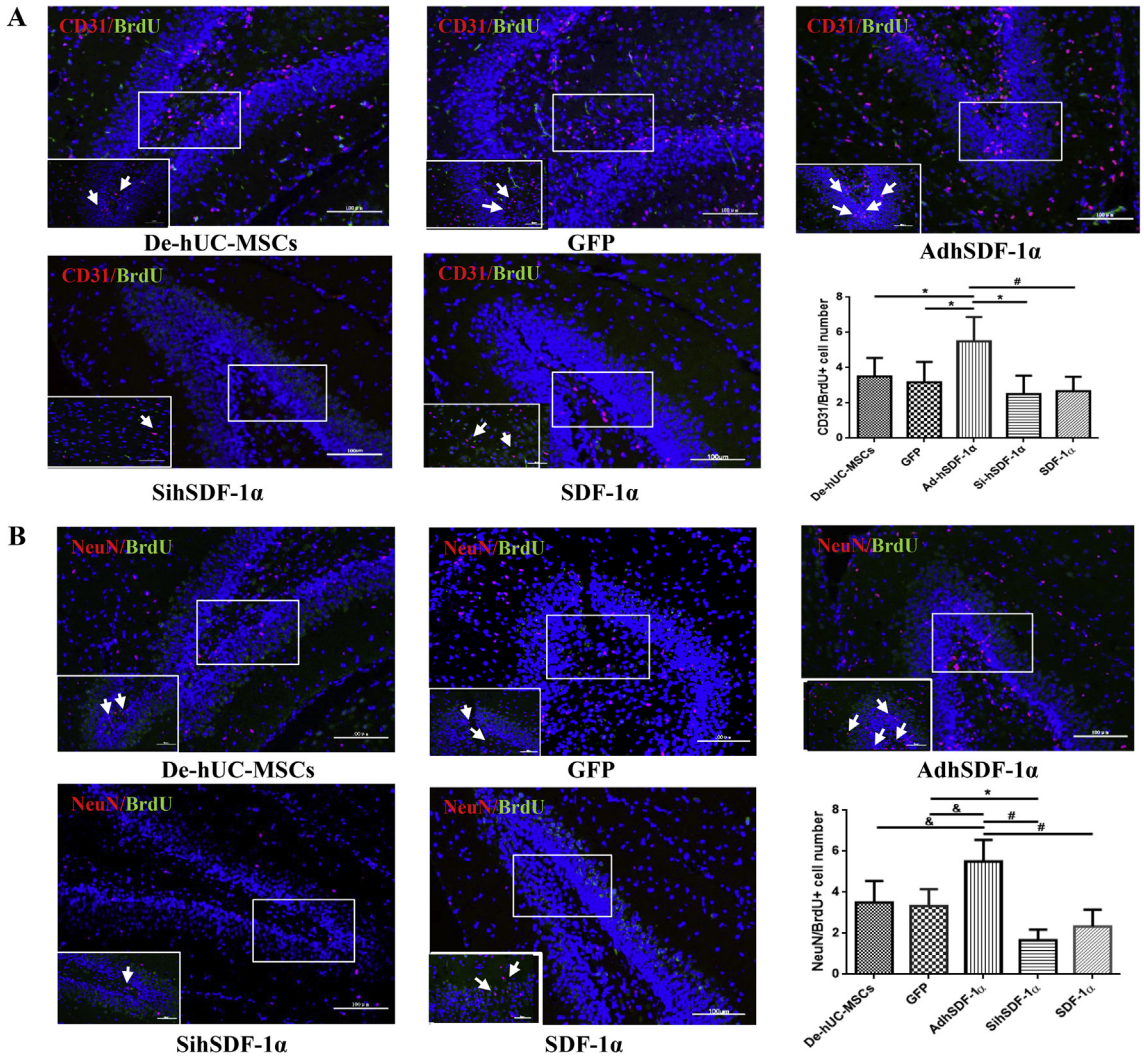

Figure 7 Immunofluorescence detection of neurogenesis and angiogenesis in hippocampus tissue. **(A)** $CD31^{+}/BrdU^{+}$ cells identified by immunofluorescence in the rat hippocampus following cell transplantation (scale bar = 100 μm). **(B)** The number of CD31/BrdU-positive cells in rat hippocampus tissue ($^{*}P < 0.05$, De-hUC-MSCs *vs*. AdhSDF-1α, GFP *vs*. AdhSDF-1α, and AdhSDF-1α *vs*. SihSDF-1α; $^{\#}P < 0.001$, AdhSDF-1α *vs*. SDF-1α; one-way ANOVA). **(C)** NeuN and BrdU double-labeled cells in the hippocampus detected via immunofluorescence (scale bar = 100 μm). **(D)** Quantitative analysis of the number of NeuN+/BrdU+ cells ($^{\&}P < 0.01$, De-hUC-MSCs *vs*. AdhSDF-1α and GFP *vs*. AdhSDF-1α; $^{\#}P < 0.001$, AdhSDF-1α *vs*. SihSDF-1α and AdhSDF-1α *vs*. SDF-1α; $^{*}P < 0.05$, GFP *vs*. SihSDF-1α; one-way ANOVA).

with our study, we consider two questions: how the endogenous hSDF-1α secreted by De-hUC-MSCs plays a neuroprotective role in rats? Why does the exogenous introduction of SDF-1α not play a role? To answer these questions, we blasted the rSDF-1α (rat stromal cell-derived factor-1) and hSDF-1α gene sequence and found that they have high homology. Thus, we speculated that hSDF-1α can also promote the downstream cascade of biological functions and signaling pathways, similar to rSDF-1α. On the other hand, endogenous hSDF-1α secreted by De-hUC-MSCs has greater biological activity than exogenous SDF-1α, indicating that De-hUC-MSCs and hSDF-1α play a synergistic role in promoting nerve repair. To further explore the signaling pathways, we detected CXCR4 and PI3K/Akt signaling pathway proteins and found that CXCR4, p-PI3K, and p-Akt were differentially expressed in the AdhSDF-1α and SihSDF-1α groups, suggesting that endocrine hSDF-1α secreted by De-hUC-MSCs may mediate the CXCR4/PI3K/Akt signaling pathway, which participates in neurovascular protection (Fig. 8).

In conclusion, we demonstrate that De-hUC-MSCs can improve learning and memory recovery in HIBD rats and that the advanced protective function is mediated by reprogramming to elicit high expression of endogenous hSDF-1α, perhaps via the CXCR4/PI3K/Akt pathway.

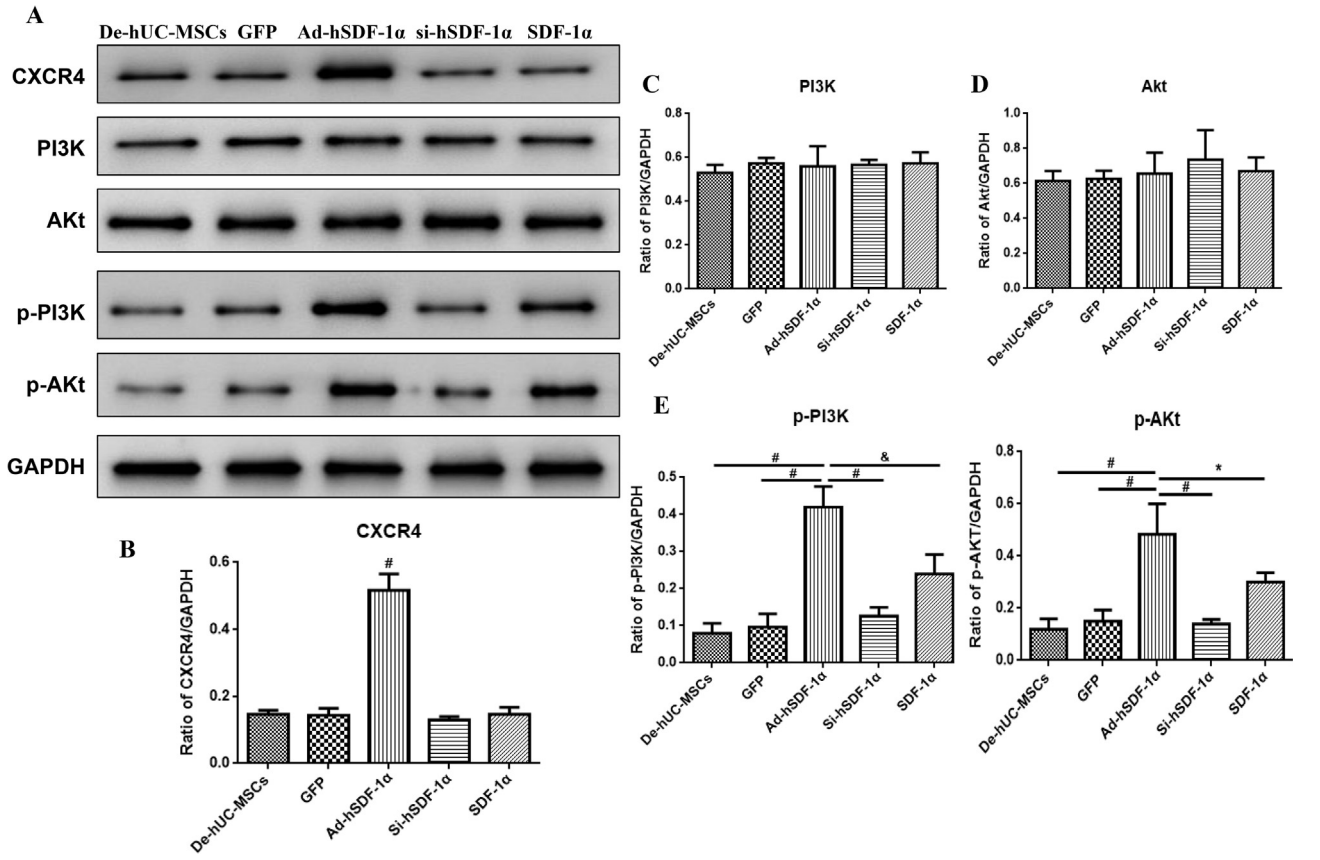

Figure 8 The CXCR4/PI3K/Akt pathway participates in the regulation mechanism. **(A)** Western blot analysis showing the expression of CXCR4, PI3K, Akt, p-PI3K, p-Akt, and GAPDH in the De-hUC-MSC, GFP, AdhSDF-1α, SihSDF-1α and SDF-1α groups. **(B—F)** Analysis of the gray value of CXCR4 ($^{\#}P < 0.001$, AdhSDF-1α *vs*. De-hUC-MSCs, GFP, SihSDF-1α and SDF-1α; one-way ANOVA), PI3K ($P > 0.05$, AdhSDF-1α *vs*. De-hUC-MSCs, GFP, SihSDF-1α and SDF-1α; one-way ANOVA), Akt ($P > 0.05$, AdhSDF-1α *vs*. De-hUC-MSCs, GFP, SihSDF-1α and SDF-1α; one-way ANOVA), p-PI3K ($^{\#}P < 0.001$, AdhSDF-1α *vs*. De-hUC-MSCs, GFP *vs*. AdhSDF-1α, and AdhSDF-1α *vs*. SihSDF-1α; $^{\&}P < 0.01$, AdhSDF-1α *vs*. SDF-1α; one-way ANOVA), p-Akt ($^{\#}P < 0.001$, AdhSDF-1α *vs*. De-hUC-MSCs, GFP *vs*. AdhSDF-1α, and AdhSDF-1α *vs*. SihSDF-1α; $^{*}P < 0.05$, AdhSDF-1α *vs*. SDF-1α; one-way ANOVA) in the five groups.

Funding

The reported work was supported by the National Natural Science of China (grant number 81601973).

Conflict of Interests

The authors have no conflicts of interest to declare.

References

1. Selway LD. State of the science: hypoxic ischemic encephalopathy and hypothermic intervention for neonates. *Adv Neonatal Care*. 2010;10(2):60—66.
2. Filippi L, Fiorini P, Daniotti M, et al. Safety and efficacy of topiramate in neonates with hypoxic ischemic encephalopathy treated with hypothermia (NeoNATI). *BMC Pediatr*. 2012;12, e144.
3. Zhou X, Gu J, Gu Y, et al. Human umbilical cord-derived mesenchymal stem cells improve learning and memory function in hypoxic-ischemic brain-damaged rats via an IL-8-mediated secretion mechanism rather than differentiation pattern induction. *Cell Physiol Biochem*. 2015;35(6):2383—2401.
4. McDonald CA, Djuliannisaa Z, Petraki M, et al. Intranasal delivery of mesenchymal stromal cells protects against neonatal hypoxic-ischemic brain injury. *Int J Mol Sci*. 2019;20(10), e2449.
5. Zhang J, Yang C, Chen J, et al. Umbilical cord mesenchymal stem cells and umbilical cord blood mononuclear cells improve neonatal rat memory after hypoxia-ischemia. *Behav Brain Res*. 2019;362:56—63.
6. Liu X, Ye R, Yan T, et al. Cell based therapies for ischemic stroke: from basic science to bedside. *Prog Neurobiol*. 2014;115:92—115.
7. Park HW, Kim Y, Chang JW, et al. Effect of single and double administration of human umbilical cord blood-derived mesenchymal stem cells following focal cerebral ischemia in rats. *Exp Neurobiol*. 2017;26(1):55—65.
8. Xie B, Gu P, Wang W, et al. Therapeutic effects of human umbilical cord mesenchymal stem cells transplantation on hypoxic ischemic encephalopathy. *Am J Transl Res*. 2016;8(7):3241—3250.
9. Guo J, Wang H, Hu X. Reprogramming and transdifferentiation shift the landscape of regenerative medicine. *DNA Cell Biol*. 2013;32(10):565—572.
10. Eguizabal C, Montserrat N, Veiga A, Izpisua Belmonte JC. Dedifferentiation, transdifferentiation, and reprogramming: future directions in regenerative medicine. *Semin Reprod Med*. 2013;31(1):82—94.

11. Yang FY, Zhang XH, Tsang LL, Chan HC, Jiang XH. Dedifferentiation-reprogrammed mesenchymal stem cells for neonates with hypoxic-ischaemic brain injury. *Hong Kong Med J*. 2019;25(4):12—16.
12. Zhang Y, Zhong JF, Qiu H, MacLellan WR, Marbán E, Wang C. Epigenomic reprogramming of adult cardiomyocyte-derived cardiac progenitor cells. *Sci Rep*. 2015;5, e17686.
13. Rice 3rd JE, Vannucci RC, Brierley JB. The influence of immaturity on hypoxic-ischemic brain damage in the rat. *Ann Neurol*. 1981;9(2):131—141.
14. Grafi G. The complexity of cellular dedifferentiation: implications for regenerative medicine. *Trends Biotechnol*. 2009;27(6):329—332.
15. Matsumoto T, Kano K, Kondo D, et al. Mature adipocyte-derived dedifferentiated fat cells exhibit multilineage potential. *J Cell Physiol*. 2008;215(1):210—222.
16. Kleiderman S, Gutbier S, Ugur Tufekci K, et al. Conversion of nonproliferating astrocytes into neurogenic neural stem cells: control by FGF2 and interferon-γ. *Stem Cell*. 2016;34(12):2861—2874.
17. Jumabay M, Matsumoto T, Yokoyama S, et al. Dedifferentiated fat cells convert to cardiomyocyte phenotype and repair infarcted cardiac tissue in rats. *J Mol Cell Cardiol*. 2009;47(5):565—575.
18. Mikrogeorgiou A, Sato Y, Kondo T, et al. Dedifferentiated fat cells as a novel source for cell therapy to target neonatal hypoxic-ischemic encephalopathy. *Dev Neurosci*. 2017;39(1—4):273—286.
19. Ullah M, Sittinger M, Ringe J. Transdifferentiation of adipogenically differentiated cells into osteogenically or chondrogenically differentiated cells: phenotype switching via dedifferentiation. *Int J Biochem Cell Biol*. 2014;46:124—137.
20. Ullah M, Stich S, Notter M, Eucker J, Sittinger M, Ringe J. Transdifferentiation of mesenchymal stem cells-derived adipogenic-differentiated cells into osteogenic- or chondrogenic-differentiated cells proceeds via dedifferentiation and have a correlation with cell cycle arresting and driving genes. *Differentiation*. 2013;85(3):78—90.
21. Yang H, Feng G-D, Olivera C, Jiao X-Y, Vitale A, Gong J, Yo S-W. Sonic hedgehog released from scratch-injured astrocytes is a key signal necessary but not sufficient for the astrocyte dedifferentiation. *Stem Cell Res*. 2012;9:156—166.
22. Xu Y, Zhang JA, Xu Y, et al. Antiphotoaging effect of conditioned medium of dedifferentiated adipocytes on skin in vivo and in vitro: a mechanistic study. *Stem Cell Dev*. 2015;24(9):1096—1111.
23. Chen R, Lee WY, Zhang XH, et al. Epigenetic modification of the CCL5/CCR1/ERK axis enhances glioma targeting in dedifferentiation-reprogrammed BMSCs. *Stem Cell Rep*. 2017;8(3):743—757.
24. Li Y, Chang S, Li W, et al. cxcl12-engineered endothelial progenitor cells enhance neurogenesis and angiogenesis after ischemic brain injury in mice. *Stem Cell Res Ther*. 2018;9(1):139.
25. Cheng X, Wang H, Zhang X, et al. The role of SDF-1/CXCR4/CXCR7 in neuronal regeneration after cerebral ischemia. *Front Neurosci*. 2017;11, e590.
26. Cui L, Qu H, Xiao T, Zhao M, Jolkkonen J, Zhao C. Stromal cell-derived factor-1 and its receptor CXCR4 in adult neurogenesis after cerebral ischemia. *Restor Neurol Neurosci*. 2013;31(3):239—251.
27. Ma J, Liu N, Yi B, et al. Transplanted hUCB-MSCs migrated to the damaged area by SDF-1/CXCR4 signaling to promote functional recovery after traumatic brain injury in rats. *Neurol Res*. 2015;37(1):50—56.
28. Shen C, Lie P, Miao T, et al. Conditioned medium from umbilical cord mesenchymal stem cells induces migration and angiogenesis. *Mol Med Rep*. 2015;12(1):20—30.
29. Gu Y, He M, Zhou X, et al. Endogenous IL-6 of mesenchymal stem cell improves behavioral outcome of hypoxic-ischemic brain damage neonatal rats by supressing apoptosis in astrocyte. *Sci Rep*. 2016;6, e18587.
30. Kim DH, Lee D, Chang EH, et al. GDF-15 secreted from human umbilical cord blood mesenchymal stem cells delivered through the cerebrospinal fluid promotes hippocampal neurogenesis and synaptic activity in an Alzheimer's disease model. *Stem Cell Dev*. 2015;24(20):2378—2390.